

# Discovery of a 26.2 day period in the long-term X-ray light curve of SXP 1323: a very short orbital period for a long spin period pulsar

S. Carpano<sup>1</sup>, F. Haberl<sup>1</sup>, and R. Sturm<sup>1</sup>

Max-Planck-Institut für extraterrestrische Physik, Giessenbachstrasse 1, 85748 Garching, Germany  
e-mail: scarpano@mpe.mpg.de

11 April 2017

## ABSTRACT

**Context.** About 120 Be/X-ray binaries (BeXBs) are known in the Small Magellanic Cloud (SMC); about half of them are pulsating with periods from a few to hundreds of seconds. SXP 1323 is one of the longest-period pulsars known in this galaxy.

**Aims.** SXP 1323 is in the field of view of a large set of calibration observations that we analyse systematically, focusing on the time analysis, in search of periodic signals.

**Methods.** We analyse all available X-ray observations of SXP 1323 from Suzaku, XMM-Newton, and Chandra, in the time range from 1999 to the end of 2016. We perform a Lomb-Scargle periodogram search in the band 2.5–10 keV on all observations to detect the neutron star spin period and constrain its long-term evolution. We also perform an orbital period search on the long-term light curve, merging all datasets.

**Results.** We report the discovery of a  $26.188 \pm 0.045$  d period analysing data from Suzaku, XMM-Newton, and Chandra, which confirms the optical period derived from the Optical Gravitational Lensing Experiment (OGLE) data. If this corresponds to the orbital period, this would be very short with respect to what is expected from the spin/orbital period relationship. We furthermore report on the spin period evolution in the last years. The source is spinning-up with an average rate of  $|\dot{P}/P|$  of  $0.018$  yr $^{-1}$ , decreasing from  $\sim 1340$  to  $\sim 1100$  s, in the period from 2006 to the end of 2016, which is also extreme with respect to the other Be/X-ray pulsars. From 2010 to the end of 2014, the pulse period is not clearly detectable, although the source was still bright.

**Conclusions.** SXP 1323 is a peculiar BeXB due to its long pulse period, rapid spin-up for several years, and short orbital period. A continuous monitoring of the source in the next years is necessary to establish the long-term behaviour of the spin period.

**Key words.** galaxies: individual: Small Magellanic Could – stars: neutron – X-rays: binaries – X-rays: individual: SXP 1323 –stars: emission-line, Be

## 1. Introduction

Be/X-ray binaries (BeXBs) belonging to the class of High-Mass X-ray binaries (HMXBs) are composed of a Be star and a compact object, generally a neutron star. In those systems, it is believed that mass transfer occurs from the equatorialcretion disc around the donor star, onto the compact object during the periastron passage of the neutron star in an eccentric orbit, either via an accretion disk or via wind capture. In this class of object, the pulse period is generally well correlated to the orbital period as reported initially by Corbet (1984, 1986), although with large scatter. The second group of HMXBs are the supergiant X-ray binaries, where the massive companion is an evolved star in which matter is transferred to the compact object via a strong wind.

A large number of BeXBs have been reported so far in the Small Magellanic Cloud (SMC) (Coe & Kirk 2015; Haberl & Sturm 2016). Galache et al. (2008) monitored 41 BeXB systems in the SMC over nine years using RXTE Proportional Counter Array (PCA) data in search of orbital modulations. They confirmed and refined ten known orbital ephemerides and determined ten new ones. More recently, Klus et al. (2014) reported the long-term average spin period of 42 BeXB systems, using RXTE data, claiming they all contain a neutron star accreting via a disc rather than a wind.

SXP 1323 is a pulsar discovered by Haberl & Pietsch (2005), and it shows one of the longest pulse periods known in the SMC.

Schmidke & Cowley (2006a,b) reported the discovery of several strong periodic signals in the optical light curve of SXP 1323, using Optical Gravitational Lensing Experiment (OGLE) data. The optical light is coming from the Be star itself, the decrection disk and transient accretion disk around the neutron star. Three strong peaks were discovered at periods of 0.41 d, 0.88 d, and 26.16 d, all showing approximatively sinusoidal light curves. The first two are believed to come from non-radial pulsations of the Be star. Later, Bird et al. (2012), analysed the OGLE light curves of 49 SMC BeXBs, and confirmed the period at 26.17 d. Authors of both papers conclude that the short periods and sinusoidal shapes are not characteristic of an orbital modulation of a decrection disc, and explain the 26.2 d period with the aliasing of non-radial pulsations at a period of 0.96 d.

## 2. Observations and data reduction

SXP 1323 is very close to the bright supernova remnant (SNR) 1E 0102-72.3, which is often observed for calibration purposes (see e.g. Plucinsky et al. 2008, 2017). A large number of observations of the source are therefore available from several X-ray observatories.

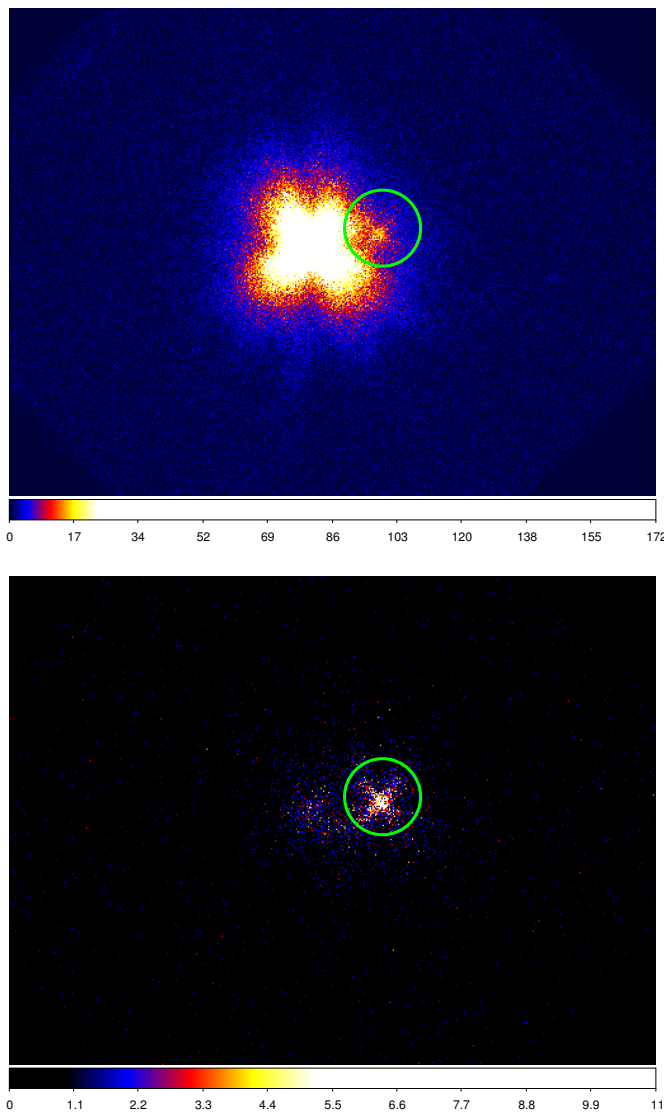


Fig. 1: Suzaku images (in counts) of the SNR 1E 0102-72.3 (ob-ID: 101005050), in the full energy band (top) where the pulsar and the SNR are confused, and in the 2.5-10 keV band (bottom) where the contribution of the SNR is negligible.

## 2.1. Suzaku observations

1E 0102-72.3 has been observed 75 times with Suzaku (Mitsuda et al. 2007), between August 2005 and April 2015 with the X-Ray Imaging Spectrometer (XIS) instrument (Koyama et al. 2007). We performed a period search on 70 XIS datasets having a total exposure time longer than 15 ks and we use all events from cleaned event files read out in 3x3 and 5x5 modes. A summary of all datasets used in this analysis is given in Table A.1. The first, second, and third columns give the observation ID, the instrument name (XIS0, XIS1, XIS2 and XIS3), and the readout mode (3x3 or 5x5 pixels read around the centre of each event), respectively. The following three columns give the date of the start of the observations, the time elapsed from the beginning to the end of the observation (in seconds) and the exposure time (in seconds), taken from the ONTIME keyword. In the full energy band, the light of the standard candle SNR 1E 0102-72.3 and the pulsar are confused. However, if events are filtered, with energies

>2.5 keV, the contribution of the SNR is negligible, as shown in Fig. 1.

## 2.2. XMM-Newton observations

Currently, 48 XMM-Newton (Jansen et al. 2001) observations are available for SNR 1E 0102-72.3. For two of them no European Photon Imaging Camera (EPIC) data are available, leaving 46 datasets with exposures from ~14 to 69 ks performed between April 2000 and December 2016. Only exposures recorded in imaging mode and with the source in the field of view are analysed. Table A.2 reports a summary of all observations used in this work.

For the event filtering, single to double and single to quadruple events are used for pn (Strüder et al. 2001) and Metal-Oxide-Silicon (MOS) (Turner et al. 2001) cameras respectively, all with FLAG=0.

## 2.3. Chandra observations

The pulsar is visible in 201 observations performed with Chandra's Advanced CCD Imaging Spectrometer (ACIS) instrument (Garmire et al. 2003), on the SNR. Those data were recorded from August 1999 to March 2016 and the datasets used in this paper are listed in Table A.3. Events from observations performed on the same day or on two consecutive days were merged together, leaving 66 independent datasets (see column 1 of Table A.3). Columns 2 and 3 give the observation ID, the operating ACIS CCDs (0-3 are I0-I3 and 4-9 are S0-S5). From 2008, the source is not in the field-of-view for most observations since only one detector was used to observe 1E 0102-72.3.

## 3. Analyses and results

The source extraction region is centred on coordinates RA, DEC= 01:03:37.8, -72:01:33, extracted from the Two Micron All Sky Survey (2MASS) catalogue (Cutri et al. 2003), with a radius of 62.5'' for Suzaku and 30'' for XMM-Newton. For Chandra the radius was 7.4'', 12.3'', 24.6'' depending on the off-axis angle of the source. For the background region, for XMM-Newton and Chandra, we use an annulus centred on the source, both with an inner and outer radius of, for XMM-Newton,  $r_{\text{in}}, r_{\text{out}} = 25'', 40''$  and for Chandra, depending on the position of the source in the field of view:  $r_{\text{in}}, r_{\text{out}} = 7.4'', 14.8'', r_{\text{in}}, r_{\text{out}} = 12.3'', 24.6''$  or  $r_{\text{in}}, r_{\text{out}} = 24.6'', 39.6''$ . On the other hand, in the case of Suzaku, the background region was not centred around the pulsar coordinates because of a potential contamination from the nearby SNR due to the large extraction region. Instead it is centred for most of the observations around coordinates RA, DEC= 01:02:56, -72:00:57, with a radius of 62.5'' (another region is chosen when this one is out of the field of view).

### 3.1. Pulse period search

The pulse period search was performed using Lomb-Scargle periodogram analysis (Lomb 1976; Scargle 1982), in the energy band 2.5–10 keV where the signal-to-noise ratio for the emission of the pulsar is maximised, and in the period range 900–1600 s. The light curves are barycenter-corrected, background-subtracted and binned to 50 s. In the case of XMM-Newton and Suzaku, events recorded by the different instruments are merged together. However, when one or more instrument is not operating for some time interval discontinuities appear in the light

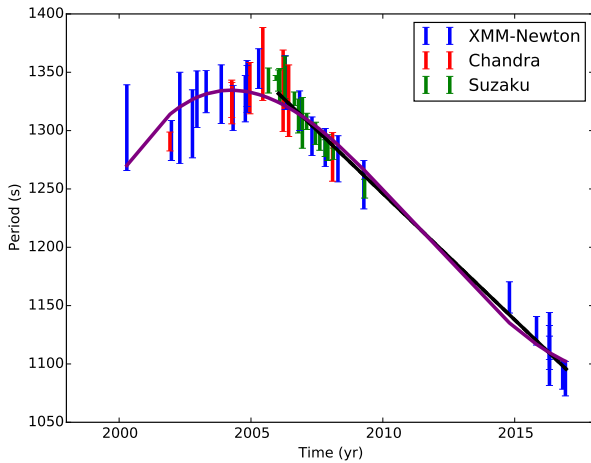


Fig. 2: Long-term spin period evolution observed with Suzaku (green), XMM-Newton (blue) and Chandra (red) data. The dotted black line is the result of a linear fit performed on data from 2006 to 2017.

curves. We correct for those effects by multiplying the portions of the light curves not covered by all cameras, by some factor, assuming that, in the 2.5–10.0 keV band, the effective area of the XMM-Newton pn camera is about 3.2 times larger than the MOS ones, and that the effective area of Suzaku’s front illuminated cameras (XIS0, XIS2 and XIS3) is about 1.1 times larger than the back illuminated one (XIS1). The uncertainties on the period are measured by fitting a Gaussian function with the Python module `astropy.modeling.Gaussian1D`. The error bars correspond to the  $1-\sigma$  standard deviation of the Gaussian.

To calculate the confidence levels, since the noise is not purely white photon noise, but also contains some red/correlated component, we proceed in the following way:

1. We divide light curves into blocks of maximum 1000 s for Chandra and XMM-Newton, and of 4000 s for Suzaku (for which observations are lasting much longer), ensuring that at least ten blocks are present per light curve.
2. We shuffle the different blocks randomly, perform a Lomb-Scargle period search and determine the maximal power of the corresponding periodogram.
3. We repeat the 2nd step 1000 times and, by collecting the maxima of all periodograms, we derive the confidence levels.

Results of the spin period search are shown in Fig. 2, for Suzaku (green), XMM-Newton (blue), and Chandra (red) data. Only periods with significance above 99% are shown. From 2002 to 2006 the pulse period seems to have increased slightly, although error bars are relatively large. This spin-down trend is in contradiction with the slow spin-up trend reported by Klus et al. (2014) who analysed RXTE data in roughly the same time interval.

From 2006 to end 2016, the source is rapidly spinning up at a rate of  $\dot{P} = -21.65 \text{ s yr}^{-1}$ . This value was calculated by fitting a line using the `numpy.polyfit` function in Python (shown as a black dotted line in Fig. 2). Using the mean value of 1216 s in the 2005–end 2016 time interval, the relative spin period change becomes:  $|\dot{P}/P| = 0.0178 \text{ s yr}^{-1} \text{ s}^{-1}$ . Alternatively, we tried to fit a 3rd degree polynomial (in purple) that takes into account the data before 2005 as well, while a 2nd degree polynomial alone would not fit the data well. From 2010 to the end of 2014, the pulse

period is only occasionally detected, but at a lower confidence level.

### 3.2. The orbital period search

The search for the orbital period was made using all available observations from Suzaku, XMM-Newton and Chandra merged together and a period search was performed in the range from 10 to 50 d. Differences in the effective area from the various instruments and vignetting issues had to be taken into account. We therefore created a simulated spectrum for the source in every observation, using `XSPEC` and the `fakeit` command and using the relevant response files. The model spectrum is the one described in Section 3.3, with  $N_{\text{H}}$  value of  $0.5 \times 10^{22} \text{ cm}^{-2}$  and  $\Gamma = 0.7$ . The count rate extracted in the 2.5–10 keV band, from all spectra, is recorded and then used to scale the different light curve segments, since these represent the values expected for a constant source. We note that, for every observation, we extract and scale the expected count rates as if all instruments were always operating (pn, MOS1 and MOS2 for XMM-Newton, and XIS0, XIS1, XIS2 and XIS3 for Suzaku). We then divide, for each observation, the measured count rate by its theoretical counterpart and multiply by a single factor to get values expected for XMM-Newton (pn+MOS1+MOS2). The results are shown in Fig. 3, where the total background-subtracted and barycenter-corrected light curve is shown at the top, the Lomb-Scargle periodogram in the middle and the folded light curve with sinusoidal fit at the bottom. A clear peak is found at a period of 26.188 d and a  $1-\sigma$  uncertainty of 0.045 d is determined from the width of the Gaussian fit on the peak. Phase 0 of the sine function is at  $\text{MJD}=51417.1695288 \pm N \times 26.188 \pm 0.045$ , where  $N$  is an integer (maximum is at phase 0.75). To calculate the significance levels we again use the bootstrap method but this time we randomly shuffle the whole light curves of all observations, again 1000 times.

### 3.3. Spectral changes with orbital period

Because of its higher sensitivity, XMM-Newton data are analysed to search for any change in the X-ray spectra with the orbital modulation. We extracted a source and background spectrum for each observation and exposure separately using standard SAS tasks. We fit the data, in the 0.3–10 keV energy band, with `XSPEC` using a power-law emission component and two absorption components (`phabs*vphabs*power`). The first absorption component has a fixed Galactic  $N_{\text{H}}$  value of  $5.36 \times 10^{20} \text{ cm}^{-2}$  (Dickey & Lockman 1990) and the second  $N_{\text{H}}$  is left free, while the abundance is fixed to 1.0 for He and 0.2 for  $Z > 2$  (Russell & Dopita 1992). Sometimes a faint soft excess ( $< 1 \text{ keV}$ ) is observed but because this component is not well constrained, we use only the power-law component to model the spectrum.

The results of the spectral fits are shown in Fig. 4. The plot at the top shows the observed 0.3–10 keV flux as a function of the orbital phase; errors are given at 68% confidence level. From those plots we can observe a variation of the flux with the orbital phase (phase 0 is the same as for the merged data in Fig. 3, that is,  $\text{MJD}=51417.1695288$ ). In the second and third plots, values of  $\Gamma$  for the power-law component and  $N_{\text{H}}$  for the absorption component are shown, as a function of the flux.

Fitting a linear relation between the parameters and the flux, gives slopes of  $-0.11 \times 10^{12} \text{ erg}^{-1} \text{ s cm}^2$  for the  $\Gamma$  and  $-0.30 \times 10^{34} \text{ erg}^{-1} \text{ s}$  for the  $N_{\text{H}}$  although there is a larger scatter in the latter plot, indicating that there is an anti-correlation between the

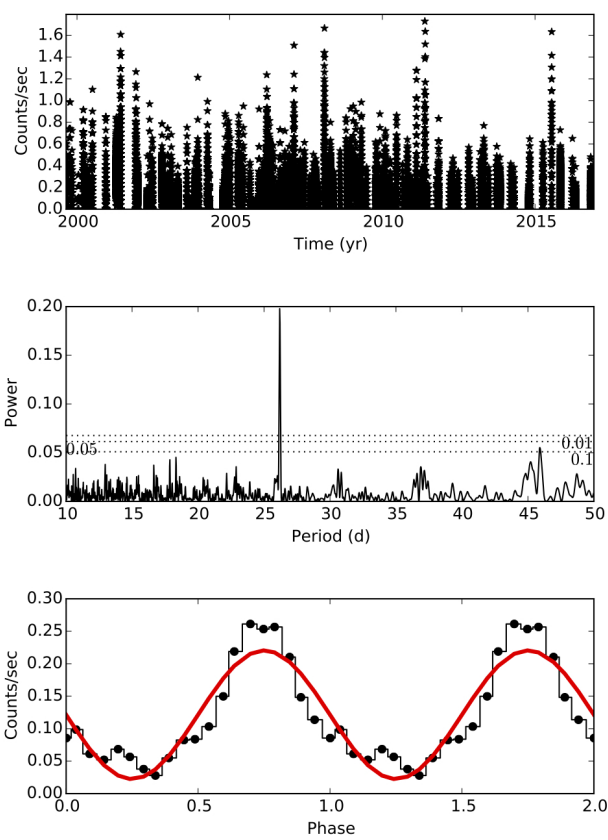


Fig. 3: Top: merging of all Suzaku, XMM-Newton, and Chandra observations as described in section 2 (arbitrary scale). Middle: Lomb-Scargle periodogram on all observations, performed over a period range of 10 to 50 d with a peak at 26.19 d. Bottom: folded light curve with fitted sine function.

power law index and the flux (the source getting harder at higher fluxes) and between the absorption and the flux (less absorption at higher fluxes), and hence with the orbital period.

#### 4. Discussion

From the analysis of XMM-Newton, Suzaku, and Chandra data it appears that SXP 1323 is a quite atypical BeXB. First, it has a long pulse period, with a very high derivative, and as described in Sec 3.1, from 2006 to the end of 2016, the neutron star is spinning up at a very rapid average rate:  $|\dot{P}/P|=0.018 \text{ s yr}^{-1} \text{ s}^{-1}$ . This is much higher than for any other SMC BeXB reported by Klus et al. (2014) in their Table 4. From 2010 to the end of 2014, the pulse period is no longer clearly detected. Such rapid spin-up and temporary apparent pulsation disappearance for several years has also been reported by Townsend et al. (2013) on SXP 91.1 using RXTE data. In their Fig. 6, they report a spin period changing linearly from 91.1 s to 85.4 s in approximatively 13.5 yrs. A linear fit provided a spin-up rate of  $\dot{P} = 1.442 \times 10^{-8} \text{ s s}^{-1}$ . Dividing by the average period (88.45 s), and changing units leads to  $|\dot{P}/P|=0.005 \text{ s yr}^{-1} \text{ s}^{-1}$ , which is still smaller than what we derived for SXP 1323. From MJD  $\sim 52500$  to  $\sim 55200$ , that is, for about 8 yrs, no pulse period could be found for SXP 91.1. The

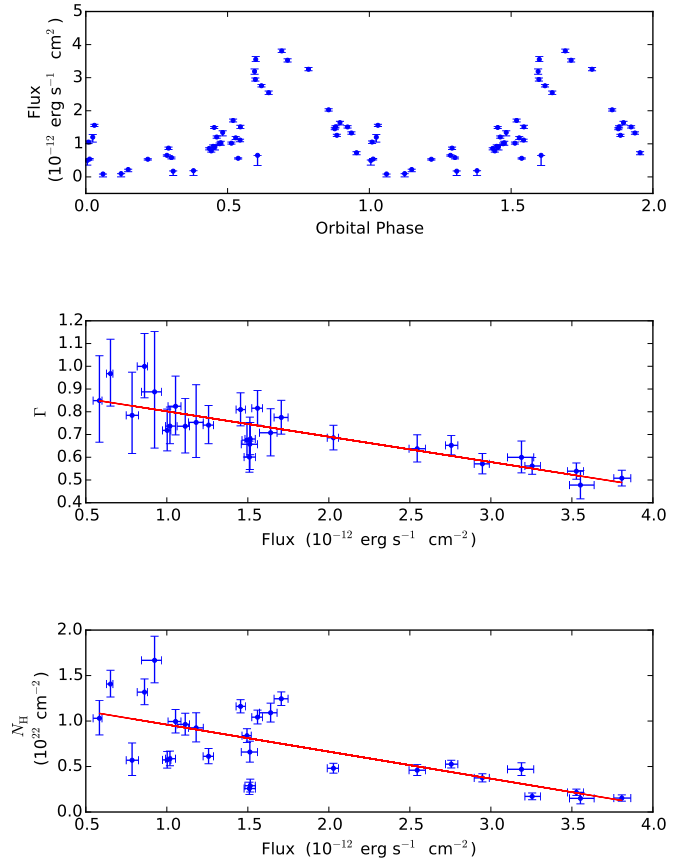


Fig. 4: 0.3–10 keV fluxes derived from spectral fits for XMM-Newton (top) as a function of orbital phase (phase 0 is the same as for the merged data). Best fitted  $\Gamma$  value for the power-law component (middle) and  $N_{\text{H}}$  for the absorption (bottom) as a function of flux.

authors suggest that the source is continuously accreting matter, and that it is unlikely that the source stopped to pulse for many years. Instead there might be nearby absorbing material preventing the pulsed X-ray emission from reaching the observer, or there might be a change in the geometry. This could easily be concluded for SXP 1323 as well.

A second peculiarity of the pulsar reported here, SXP 1323, is the very short 26.2 d period detected in X-rays and optical wavelengths compared to the long pulse period. While the 26.2 d optical period has been explained so far by aliases of non-radial pulsations of the Be star, this is no longer possible due to the detection of the same period in X-rays. Although we cannot exclude other possibilities for the X-ray variability, we don't know of any plausible explanation which is not related to the orbital period. Such a short orbital period does not follow the spin-orbit period relationship reported by Corbet (1984, 1986), although there is a large scatter of the observed systems for this relation. From Eq. 1, in Corbet (1986), a pulse period of 1323 s would lead to an orbital period of 364 d for circular orbit, and higher for an eccentric orbit. This relationship assumes that the neutron star is in a state of quasi-equilibrium in which the Alfvén and corotation radii are equal on average. Other exceptions to this rule are observed for BeXBs in the SMC, although these are

less extreme cases than SXP 1323. Some examples with  $P_{\text{spin}} > 100$  s and  $P_{\text{orb}} < 50$  d are SXP 264 (Haberl & Pietsch 2004) with an orbital period of 49.1 d (Schmidtke & Cowley 2005); SXP 325 (Haberl et al. 2008) with an orbital period of 45.995 d (Coe et al. 2008); SXP 214 (Coe et al. 2011) with an orbital period of 29.91 d (Schmidtke et al. 2013); and SXP 101 (Yokogawa et al. 2000) with an orbital period of 21.94 (McGowan et al. 2007). All orbital periods were derived using optical data from OGLE and in some cases from the Massive Astrophysical Compact Halo Object (MACHO) project as well. In our Galaxy, some other comparable systems are: 1A 1118-616, with a pulse period of 405 s and an orbital period of 24.0 d (Staubert et al. 2011) determined using RXTE data, and, SAX J2103.5+4545 with a pulse period of 358.6 s, which is the BeXB with the shortest known orbital period of 12.7 d (Reig et al. 2004) determined using RXTE data as well. They occupy the region of the wind-fed supergiant binaries in the  $P_{\text{spin}} - P_{\text{orb}}$  diagram. Reig et al. (2010) suggest that the X-rays observed during the quiescence state of SAX J2103.5+4545 are more likely the result of wind accretion. The dominant accretion wind is likely coming from a more stable equatorial low-velocity high-density wind from the Be star, since, in contrast to wind-fed systems with supergiants, which show erratic and flaring X-ray variability, the X-ray flux in quiescence is stable. In this scenario, the neutron star orbit is coplanar to the plane of the circumstellar disk.

Such a model could be applied to SXP 1323 as well, to explain on one hand the presence of a short orbital period and on the another hand the sinusoidal shapes of the folded X-ray and the optical light curves, as shown in this work by Schmidtke & Cowley (2006a) and Bird et al. (2012). This rather sinusoidal shape would mean that the system is not undergoing regular outbursts as commonly observed in BeXBs, but the neutron star seems to accrete continuously during its orbit around the Be star companion. Accretion from an equatorial low-velocity high-density wind could provide an explanation. Some of the SMC BeXBs with known X-ray orbital periods presented by Galache et al. (2008) also have sinusoidal shape, similar to, for example, SXP 138 ( $P_{\text{orb}}=103.6$  d) and SXP 280 ( $P_{\text{orb}}=64.8$  d) and could also be explained by this model.

## 5. Conclusions

From this work, it appears that SXP 1323 is a peculiar BeXB due to its long pulse period, rapid spin-up for several years, and short orbital period. Thanks to the nearby SNR 1E 0102-72.3, which is used as a calibration target for most CCD detectors, a large number of observations are already available for this source allowing a study of the long-term behaviour of the pulse period and the detection of long periodicities in X-rays. A continuous monitoring of the source in the future is necessary to determine how the pulse period will evolve in the near future.

**Acknowledgements.** The scientific results reported in this article are based on data obtained from the Chandra Data Archive, on observations obtained with XMM-Newton, an ESA science mission with instruments and contributions directly funded by ESA Member States and the USA (NASA), and on data obtained from the Suzaku satellite, a collaborative mission between the space agencies of Japan (JAXA) and the USA (NASA).

- Corbet, R. H. D. 1984, A&A, 141, 91
- Corbet, R. H. D. 1986, MNRAS, 220, 1047
- Cutri, R. M., Skrutskie, M. F., van Dyk, S., et al. 2003, VizieR Online Data Catalog, 2246
- Dickey, J. M. & Lockman, F. J. 1990, ARA&A, 28, 215
- Galache, J. L., Corbet, R. H. D., Coe, M. J., et al. 2008, ApJS, 177, 189
- Garmire, G. P., Bautz, M. W., Ford, P. G., Nousek, J. A., & Ricker, Jr., G. R. 2003, in Society of Photo-Optical Instrumentation Engineers (SPIE) Conference Series, Vol. 4851, X-Ray and Gamma-Ray Telescopes and Instruments for Astronomy., ed. J. E. Truemper & H. D. Tananbaum, 28–44
- Haberl, F., Eger, P., & Pietsch, W. 2008, A&A, 489, 327
- Haberl, F. & Pietsch, W. 2004, A&A, 414, 667
- Haberl, F. & Pietsch, W. 2005, A&A, 438, 211
- Haberl, F. & Sturm, R. 2016, A&A, 586, A81
- Jansen, F., Lumb, D., Altieri, B., et al. 2001, A&A, 365, L1
- Klus, H., Ho, W. C. G., Coe, M. J., Corbet, R. H. D., & Townsend, L. J. 2014, MNRAS, 437, 3863
- Koyama, K., Tsunemi, H., Dotani, T., et al. 2007, PASJ, 59, 23
- Lomb, N. R. 1976, Ap&SS, 39, 447
- McGowan, K. E., Coe, M. J., Schurch, M., et al. 2007, MNRAS, 376, 759
- Mitsuda, K., Bautz, M., Inoue, H., et al. 2007, PASJ, 59, 1
- Plucinsky, P. P., Beardmore, A. P., Foster, A., et al. 2017, A&A, 597, A35
- Plucinsky, P. P., Haberl, F., Dewey, D., et al. 2008, in Society of Photo-Optical Instrumentation Engineers (SPIE) Conference Series, Vol. 7011, Society of Photo-Optical Instrumentation Engineers (SPIE) Conference Series
- Reig, P., Negueruela, I., Fabregat, J., et al. 2004, A&A, 421, 673
- Reig, P., Słowińska, A., Zezas, A., & Blay, P. 2010, MNRAS, 401, 55
- Russell, S. C. & Dopita, M. A. 1992, ApJ, 384, 508
- Scargle, J. D. 1982, ApJ, 263, 835
- Schmidtke, P. C. & Cowley, A. P. 2005, AJ, 130, 2220
- Schmidtke, P. C. & Cowley, A. P. 2006a, The Astronomer's Telegram, 716, 1
- Schmidtke, P. C. & Cowley, A. P. 2006b, AJ, 132, 919
- Schmidtke, P. C., Cowley, A. P., & Udalski, A. 2013, The Astronomer's Telegram, 4936, 1
- Staubert, R., Pottschmidt, K., Doroshenko, V., et al. 2011, A&A, 527, A7
- Strüder, L., Briel, U., Dennerl, K., et al. 2001, A&A, 365, L18
- Townsend, L. J., Drave, S. P., Hill, A. B., et al. 2013, MNRAS, 433, 23
- Turner, M. J. L., Abbey, A., Arnaud, M., et al. 2001, A&A, 365, L27
- Yokogawa, J., Torii, K., Kohmura, T., Imanishi, K., & Koyama, K. 2000, PASJ, 52, L53

## Appendix A: Summary of the XMM-Newton, Chandra and Suzaku observations

## References

- Bird, A. J., Coe, M. J., McBride, V. A., & Udalski, A. 2012, MNRAS, 423, 3663
- Coe, M. J., Haberl, F., Sturm, R., et al. 2011, MNRAS, 414, 3281
- Coe, M. J. & Kirk, J. 2015, MNRAS, 452, 969
- Coe, M. J., Schurch, M., Corbet, R. H. D., et al. 2008, MNRAS, 387, 724

Table A.1: Summary of the Suzaku observations used in this work (see text for more details).

Obs ID	Instr	Mode	Date start	Telapse	Ontime	Obs ID	Instr	Mode	Date start	Telapse	Ontime
100014010	XIS0	3x3	2005-08-31T01:42:20	43384	18054	101005070	XIS0	3x3	2006-10-21T15:36:54	15064	12456
	XIS0	5x5		35163	6280		XIS0	3x3		24792	18680
	XIS1	3x3		43384	18054		XIS0	5x5		7674	6034
	XIS1	5x5		35163	6280		XIS1	3x3		15064	12440
	XIS2	3x3		43384	18054		XIS1	3x3		24792	18656
	XIS2	5x5		35163	6280		XIS1	5x5		7674	6034
	XIS3	3x3		43384	18054		XIS2	3x3		15064	12456
	XIS3	5x5		35163	6280		XIS2	3x3		24792	18680
	XIS0	3x3		289212	46991		XIS2	5x5		7674	6034
	XIS0	5x5		195874	12728		XIS3	3x3		15064	12456
100044010	XIS1	3x3	2005-12-16T01:43:08	289212	93038		XIS3	3x3		24784	18672
	XIS1	5x5		195874	12757		XIS3	5x5		7674	6034
	XIS2	3x3		289212	46991	101005090	XIS0	3x3	2006-12-13T18:53:16	29180	28226
	XIS2	5x5		195874	12732		XIS1	3x3		29180	28226
	XIS3	3x3		289212	46991		XIS3	3x3		29180	28226
	XIS3	5x5		195874	12730	101005100	XIS0	3x3		44089	22614
	XIS0	2x2	2006-01-17T23:22:57	12142	6885		XIS1	3x3		44089	22614
	XIS0	3x3		195295	15657		XIS3	3x3		44089	22614
	XIS0	5x5		198072	18726	101005110	XIS0	3x3		75499	36102
	XIS1	2x2		12142	6893		XIS1	3x3		75491	36094
	XIS1	3x3		86960	13623		XIS3	3x3		75499	36102
100044020	XIS1	3x3		2169	2169	101005120	XIS0	3x3	2007-03-18T21:11:19	31388	18242
	XIS1	5x5		198072	19167		XIS1	3x3		31396	18250
	XIS2	2x2		12142	6885		XIS3	3x3		31404	18258
	XIS2	3x3		195295	15681	102001010	XIS0	3x3		30202	18115
	XIS2	5x5		198072	18695		XIS1	3x3		30202	18115
	XIS3	2x2		12142	6893	102002010	XIS0	3x3		60202	19155
	XIS3	3x3		86960	13548		XIS1	3x3		25128	8717
	XIS3	5x5		2169	2169		XIS3	3x3		60202	19155
	XIS0	3x3	2006-02-02T20:19:20	198072	18751		XIS1	5x5		25128	8717
	XIS0	5x5		19746	11324		XIS3	3x3		60202	19155
100044030	XIS1	3x3		29241	9512	102003010	XIS0	3x3	2007-08-12T05:21:09	80306	39490
	XIS1	5x5		19754	11332		XIS1	3x3		80298	39482
	XIS2	3x3		29241	9512		XIS3	3x3		80306	39490
	XIS2	5x5		19754	11332	102004010	XIS0	3x3		70817	20679
	XIS3	3x3		29241	9512		XIS0	5x5		18945	5496
	XIS3	5x5		19738	11316		XIS1	3x3		70817	20679
	XIS0	3x3		29241	9512		XIS3	5x5		25128	8717
	XIS0	5x5		19754	11332		XIS3	3x3		60202	19155
	XIS1	3x3		29241	9512	102005010	XIS0	3x3		25128	8717
	XIS1	5x5		19754	11332		XIS1	5x5		60202	19155
101005010	XIS2	3x3	2006-04-16T09:42:04	43672	21340		XIS1	3x3		25128	8717
	XIS2	5x5		43672	21324		XIS3	3x3		18945	5496
	XIS3	3x3		43672	21332		XIS1	5x5		18945	5496
	XIS3	5x5		43672	21340		XIS3	3x3		18945	5496
101005020	XIS0	3x3	2006-05-21T17:16:07	36774	17238	102005010	XIS0	3x3	2007-12-01T19:25:40	51709	24767
	XIS1	3x3		36774	18194		XIS1	3x3		51717	24791
	XIS2	3x3		36774	17238		XIS3	3x3		51725	24791
	XIS3	3x3		36774	18194	102006010	XIS0	3x3		48686	26801
101005030	XIS0	3x3	2006-06-26T20:47:26	46952	17576		XIS0	5x5		3246	1438
	XIS0	5x5		18818	4140		XIS1	3x3		48686	26801
	XIS1	3x3		26221	15040		XIS1	5x5		3246	1438
	XIS1	5x5		6789	2512		XIS3	3x3		48686	26801
	XIS2	3x3		18818	3956		XIS3	5x5		3246	1438
	XIS2	5x5		46952	17576	102021010	XIS0	3x3		32517	24915
	XIS3	3x3		18818	4140		XIS1	3x3		32517	24915
	XIS3	5x5		26213	15032		XIS3	3x3		32517	24915
	XIS0	3x3		6789	2512	102022010	XIS0	3x3		37839	20970
	XIS0	5x5		18818	3956		XIS0	5x5		18148	5509
101005040	XIS1	3x3	2006-07-17T06:22:33	54584	12813		XIS1	3x3		100646	36897
	XIS0	3x3		1391	1391		XIS1	5x5		104399	11541
	XIS0	5x5		25535	7775		XIS3	3x3		37839	20970
	XIS1	3x3		54584	14228		XIS3	5x5		18148	5509
	XIS1	5x5		25535	7876	103001010	XIS0	3x3		37825	18635
	XIS2	3x3		54584	12813		XIS0	5x5		12486	3743
	XIS2	5x5		1391	1391		XIS1	3x3		37809	18619
	XIS3	3x3		25535	7775		XIS3	3x3		12486	3743
	XIS3	5x5		6789	2512		XIS3	5x5		37825	18635
	XIS0	3x3		18818	3956	103001020	XIS0	3x3		12486	3743
101005050	XIS0	5x5		26213	15032		XIS1	3x3		37825	18635
	XIS0	5x5		54576	14220		XIS1	5x5		12486	3743
	XIS1	3x3		25535	7876		XIS3	3x3		37825	18635
	XIS1	5x5		70406	33157		XIS3	5x5		12486	3743
	XIS2	3x3		54576	14220	103001030	XIS0	3x3		58075	14348
	XIS2	5x5		70406	33157		XIS0	5x5		23267	6981
	XIS3	3x3		54576	14220		XIS1	3x3		58059	14332
	XIS3	5x5		70406	33157		XIS1	5x5		23267	6981
	XIS0	3x3		3648	1526		XIS3	3x3		58075	14348
	XIS0	5x5		1846	1846		XIS3	5x5		23267	6981
101005050	XIS1	3x3		24602	7263	103001030	XIS0	3x3	2008-08-12T22:21:28	56892	16876
	XIS1	5x5		3648	1526		XIS1	3x3		17269	4434
	XIS2	3x3		68264	31279		XIS1	5x5		56892	16876
	XIS2	5x5		1846	1846		XIS3	3x3		17269	4434
	XIS3	3x3		24602	7263		XIS3	5x5		56884	16868
	XIS3	5x5		3648	1526		XIS3	5x5		17269	4434
	XIS0	3x3		3648	1526						
	XIS0	5x5		3648	1526						
	XIS1	3x3		3648	1526						
	XIS1	5x5		3648	1526						

Table A.1: (continued)

Obs ID	Instr	Mode	Date start	Telapse	Ontime	Obs ID	Instr	Mode	Date start	Telapse	Ontime
103001040	XIS0	3x3	2008-10-22T02:31:56	41072	24381	105005010	XIS0	3x3	2010-06-19T18:54:20	44296	20278
	XIS0	5x5		1024	1024		XIS1	3x3		44296	20278
	XIS1	3x3		41072	24381		XIS3	3x3		44296	20278
	XIS1	5x5		1024	1024		XIS0	3x3	2010-12-09T11:43:15	63265	16312
	XIS3	3x3		41072	24381		XIS0	5x5		23142	6159
	XIS3	5x5		1024	1024		XIS1	3x3		63265	16312
103001050	XIS0	3x3	2008-12-13T13:33:21	41409	23416		XIS1	5x5		23142	6159
	XIS0	5x5		18211	6218		XIS3	3x3		63265	16312
	XIS1	3x3		41409	23416		XIS3	5x5		23142	6159
	XIS1	5x5		18211	6218		XIS0	3x3	2010-12-07T19:16:57	104320	40729
	XIS3	3x3		41409	23400		XIS1	3x3	2010-08-29T18:28:07	93168	36454
	XIS3	5x5		18211	6218		XIS0	3x3	2011-04-11T19:52:58	31879	17288
103001060	XIS0	3x3	2009-03-09T03:07:54	42302	23860		XIS0	5x5		11504	3098
	XIS1	3x3		42302	23844		XIS1	3x3		31879	17288
	XIS3	3x3		42302	23868		XIS3	5x5		11504	3098
	XIS0	3x3	2009-04-23T15:17:13	42736	12225		XIS1	3x3		31879	17288
	XIS0	5x5		19096	7215		XIS1	5x5		11504	3098
	XIS1	3x3		82529	37813		XIS3	3x3		31879	17288
104005010	XIS1	5x5		19096	7215		XIS3	5x5		11504	3098
	XIS3	3x3		42736	12225		XIS0	3x3	2011-06-29T02:20:44	41528	28790
	XIS3	5x5		19096	7215		XIS1	3x3		41536	28798
	XIS0	3x3	2009-06-26T03:42:21	32790	21083		XIS3	3x3		41520	28782
	XIS1	3x3		32790	21083		XIS0	3x3	2011-10-14T15:30:43	29488	26701
	XIS3	3x3		32790	21083		XIS0	5x5		7796	6124
104007010	XIS0	3x3	2009-10-26T18:14:08	56690	16256		XIS1	3x3		29480	26693
	XIS0	5x5		13067	4127		XIS1	5x5		7796	6124
	XIS1	3x3		56690	16256		XIS3	3x3		29488	26701
	XIS1	5x5		13067	4127		XIS3	5x5		7796	6124
	XIS3	3x3		56682	16248		XIS0	3x3	2012-03-17T09:12:28	49361	27563
	XIS3	5x5		13067	4127		XIS0	5x5		14922	4831
104008010	XIS0	3x3	2009-10-11T14:30:55	35836	24727		XIS1	3x3		49361	27547
	XIS1	3x3		67352	41718		XIS1	5x5		14922	4831
	XIS1	5x5		37449	7923		XIS3	3x3		49361	27563
	XIS3	3x3		35836	24727		XIS3	5x5		14922	4831
	XIS0	3x3	2009-12-25T21:59:01	35015	18297		XIS0	3x3	2011-04-12T08:28:16	32188	17344
	XIS0	5x5		12010	3696		XIS0	5x5		11690	3481
104009010	XIS1	3x3		35007	18289		XIS1	3x3		32188	17344
	XIS1	5x5		12010	3696		XIS1	5x5		9203	3386
	XIS3	3x3		35015	18297		XIS3	3x3		32188	17344
	XIS3	5x5		12010	3696		XIS3	5x5		11679	3470
	XIS0	3x3	2010-02-04T17:50:39	56815	14909		XIS0	3x3	2011-04-12T21:21:13	26192	12419
	XIS0	5x5		17561	5600		XIS0	5x5		15076	4410
104011010	XIS1	3x3		56807	14901		XIS1	3x3		26192	13867
	XIS1	5x5		17561	5600		XIS1	5x5		15076	4410
	XIS3	3x3		56815	14909		XIS3	3x3		26192	13867
	XIS3	5x5		17561	5600		XIS3	5x5		15076	4410
	XIS0	3x3	2009-10-20T19:14:20	31735	14622		XIS0	3x3	2011-10-15T02:11:09	31064	26261
	XIS0	5x5		12664	4416		XIS0	5x5		7640	5304
104012010	XIS1	3x3		31735	15568		XIS3	3x3		31064	26357
	XIS1	5x5		12664	4416		XIS3	5x5		7648	5319
	XIS3	3x3		31735	15568		XIS0	3x3	2012-04-22T22:13:35	49254	26319
	XIS3	5x5		12664	4416		XIS0	5x5		12787	4151
	XIS0	3x3	2010-02-05T10:26:37	48368	23494		XIS1	3x3		49254	26287
	XIS1	3x3		48376	23502		XIS1	5x5		12787	4151
104014010	XIS3	3x3		48366	23492		XIS3	3x3		49254	26311
	XIS1	3x3	2009-12-01T21:39:19	88538	51948		XIS3	5x5		12787	4151
	XIS1	5x5		18663	10711		XIS0	3x3	2012-06-25T09:02:38	51935	26992
	XIS3	3x3		40761	21593		XIS0	5x5		16223	3736
	XIS3	5x5		40753	21593		XIS1	3x3		51935	26992
	XIS0	3x3	2010-06-19T03:06:41	53519	13148		XIS1	5x5		16222	3735
105004020	XIS0	5x5		19007	6090		XIS3	3x3		51935	26992
	XIS1	3x3		53519	13148		XIS3	5x5		16223	3736
	XIS1	5x5		19007	6090		XIS0	3x3	2012-10-29T02:53:50	51192	26841
	XIS3	3x3		53511	13140		XIS0	5x5		17724	5269
	XIS3	5x5		19007	6090		XIS1	3x3		51190	26839
	XIS0	3x3	2010-10-26T19:30:06	29894	16549		XIS1	5x5		17724	5269
105004040	XIS0	5x5		11831	4071		XIS3	3x3		51206	26834
	XIS1	3x3		29902	15948		XIS3	5x5		11724	5269
	XIS1	5x5		11831	4071		XIS0	3x3	2013-03-13T21:17:23	64330	26441
	XIS3	3x3		29910	16573		XIS0	5x5		17450	6160
	XIS3	5x5		11831	4071		XIS1	3x3		64330	26449
	XIS0	3x3	2010-12-09T00:36:56	39870	20071		XIS1	5x5		17450	6160
105004050	XIS1	3x3		37253	19985		XIS3	3x3		64330	26449
	XIS3	3x3		37237	19969		XIS3	5x5		17450	6160
	XIS0	3x3	2011-02-08T00:21:57	33863	17259		XIS0	3x3	2012-04-23T17:30:23	60725	30367
	XIS1	3x3		33847	17243		XIS0	5x5		4160	1761
	XIS3	3x3		33863	17259		XIS1	3x3		60725	30367
	XIS3	5x5		33863	17259		XIS1	5x5		4160	1761
105004060	XIS0	3x3					XIS3	3x3		60725	30367
	XIS1	3x3					XIS3	5x5		4160	1761
	XIS3	3x3					XIS0	3x3		60725	30367
	XIS3	5x5					XIS0	5x5		4160	1761
	XIS0	3x3					XIS1	3x3		60725	30367
	XIS1	3x3					XIS1	5x5		4160	1761

Table A.1: (continued)

Obs ID	Instr	Mode	Date start	Telapse	Ontime
107003020	XIS0	3x3	2012-10-29T22:40:18	54329	29143
	XIS0	5x5		60336	2108
	XIS1	3x3		54329	29143
	XIS1	5x5		60336	2108
	XIS3	3x3		54329	29143
	XIS3	5x5		60336	2108
108002010	XIS0	3x3	2013-04-27T11:03:35	66770	29345
	XIS1	3x3		64426	29323
	XIS3	3x3		66770	29337
	XIS0	3x3	2013-06-26T14:09:57	65655	23429
108002020	XIS0	5x5		23498	9715
	XIS1	3x3		65635	23427
	XIS1	5x5		23498	9715
	XIS3	3x3		65632	23424
	XIS3	5x5		23498	9715
	XIS0	3x3	2013-09-28T14:05:19	76513	25446
108002030	XIS0	5x5		23246	6513
	XIS1	3x3		76513	25446
	XIS1	5x5		23246	6513
	XIS3	3x3		76551	25448
	XIS3	5x5		23246	6513
	XIS0	3x3	2014-03-15T15:45:37	59729	29279
108002040	XIS1	3x3		59737	29279
	XIS3	3x3		59737	29287
	XIS0	3x3	2013-04-28T05:38:23	65824	27443
	XIS1	3x3		65829	30785
108003020	XIS3	3x3		65829	30785
	XIS0	3x3	2013-09-29T11:39:14	77786	33613
	XIS1	3x3		77786	33613
	XIS3	3x3		77786	33613
109001010	XIS0	3x3	2014-04-21T05:39:51	74497	24142
	XIS0	5x5		23019	6596
	XIS1	3x3		74497	24150
	XIS1	5x5		23019	6596
	XIS3	3x3		74497	24150
	XIS3	5x5		23019	6596
109001030	XIS0	3x3	2015-04-03T16:10:16	57180	27957
	XIS0	5x5		5838	1773
	XIS1	3x3		57180	27957
	XIS1	5x5		5838	1773
	XIS3	3x3		57180	27957
	XIS3	5x5		5838	1773
109002010	XIS0	3x3	2014-04-22T03:19:30	75008	24998
	XIS0	5x5		23039	6686
	XIS1	3x3		74994	24984
	XIS1	5x5		23039	6686
	XIS3	3x3		75008	24998
	XIS3	5x5		23039	6686
109002020	XIS0	3x3	2014-10-29T05:35:13	71936	17151
	XIS0	5x5		23263	6684
	XIS1	3x3		71938	24660
	XIS1	5x5		23263	6684
	XIS3	3x3		71938	24660
	XIS3	5x5		23263	6684
109003010	XIS0	3x3	2015-04-07T13:56:45	66049	31388
	XIS0	5x5		6299	2001
	XIS1	3x3		66049	31388
	XIS1	5x5		6307	2009

Table A.2: Summary of the XMM-Newton observations used in this work (see text for more details).

Obs ID	ExpID	Date start	Ontime	Filter
0123110201	PNS001	2000-04-16T19:55:28.094	19300	Thin1
	M1S003	2000-04-16T20:08:21.126	18700	Thin1
	M2S005	2000-04-16T20:08:22.126	18700	Thin1
	PNS002	2000-04-17T04:29:41.335	17240	Medium
	M1S004	2000-04-17T04:42:34.365	16637	Medium
	M2S006	2000-04-17T04:42:33.365	16645	Medium
0135720601	PNS001	2001-04-15T01:19:17.869	16004	Thin1
	PNS009	2001-04-14T21:02:04.263	12497	Thin1
	M1S003	2001-04-14T20:46:14.225	32705	Thin1
	M2S005	2001-04-14T20:46:14.225	32705	Thin1
	PNS001	2001-12-25T18:57:56.487	31265	Thin1
	M1S003	2001-12-25T18:42:00.509	32064	Thin1
0135720901	PNS001	2002-04-20T23:00:53.809	12589	Thin1
	M2S005	2002-04-20T22:27:31.728	12680	Thin1
	PNS001	2002-05-18T11:43:55.750	12026	Thin1
	PNS017	2002-05-18T15:56:39.404	13000	Thin1
	M1S018	2002-05-18T15:02:24.266	16600	Thin1
	M2S005	2002-05-18T10:40:34.580	14758	Thin1
0135721101	PNS001	2002-10-13T03:25:52.041	10199	Thin1
	PNS017	2002-10-13T06:54:57.588	10200	Thin1
	M1S003	2002-10-13T03:21:08.051	23600	Thin1
	M2S005	2002-10-13T03:21:08.051	23600	Thin1
	PNS001	2002-12-14T03:56:35.528	10900	Thin1
	PNS017	2002-12-14T07:37:18.089	14184	Thin1
0135721301	M1S003	2002-12-14T03:51:50.538	28277	Thin1
	M2S005	2002-12-14T03:51:50.538	28275	Thin1
	PNS017	2003-04-20T19:20:34.709	18685	Medium
	PNU002	2003-04-20T14:55:28.035	13599	Medium
	PNS001	2003-10-27T08:18:11.876	28292	Thick
	M1S003	2003-10-27T07:55:47.931	29894	Thin1
0135721501	M2S005	2003-10-27T07:55:47.931	29883	Thin1
	PNS001	2003-11-16T06:33:58.358	26449	Thick
	M1S003	2003-11-16T06:11:31.414	27121	Thin1
	M2S005	2003-11-16T06:11:32.414	27124	Thin1
	PNS001	2004-04-28T07:29:19.755	31643	Thick
	PNS001	2004-10-26T07:26:05.704	29517	Thick
0135721701	M1S003	2004-10-26T06:57:21.774	31520	Thin1
	M2S005	2004-10-26T06:57:21.774	31520	Thin1
	PNS001	2004-11-07T04:00:28.611	29837	Thin1
	M1S003	2004-11-07T03:38:04.665	31439	Thin1
	M2S005	2004-11-07T03:38:03.665	31428	Thin1
	PNS001	2004-11-07T13:28:47.166	10466	Thin2
0135722201	PNU014	2004-11-07T16:36:10.671	5215	Thin1
	PNU027	2004-11-07T18:15:45.405	8298	Thin2
	M1U002	2004-11-07T13:09:48.216	22470	UNDEF.
	M1U003	2004-11-07T21:15:26.919	2200	UNDEF.
	M2S005	2004-11-07T13:06:22.225	22764	Thin1
	M2U002	2004-11-07T21:18:01.912	2100	Thin1
0135722301	PNS001	2004-11-07T22:58:08.619	26842	Thin1
	M1S003	2004-11-07T22:35:43.681	31313	Thin1
	M2U002	2004-11-07T22:44:54.656	30761	UNDEF.
	PNS001	2004-10-14T09:10:52.339	30522	Thick
	M1S003	2004-10-14T09:05:26.352	30719	Thick
	M2S005	2004-10-14T09:05:26.352	30729	Thick
0135722401	PNS001	2005-04-17T22:43:29.224	34719	Thin1
	M1S003	2005-11-05T06:50:36.089	29947	Medium
	M1S003	2005-11-05T06:45:10.103	30146	Thin1
	M2S005	2005-11-05T06:45:11.103	30143	Thin1
	PNS001	2006-04-20T02:29:36.236	30000	Thin1
	M1S003	2006-04-20T02:24:10.223	30200	Thin1
0412980101	M2S005	2006-04-20T02:24:09.223	30200	Thin1
	PNS001	2006-11-05T01:00:54.354	31868	Medium
	M1S002	2006-11-05T00:55:28.365	32065	Thin1
	M2S003	2006-11-05T00:55:28.365	32074	Thin1
	PNS001	2007-04-25T12:41:15.764	35867	Thin1
	M1S002	2007-04-25T12:35:49.748	36062	Thin1
0412980201	M2S003	2007-04-25T12:35:49.748	36070	Thin1
	PNS001	2007-10-26T09:55:18.821	36593	Medium
	M1S002	2007-10-26T09:49:52.834	36795	Thin1
	M2S003	2007-10-26T09:49:52.834	36794	Thin1

**Notes.** Columns 1 to 5 show the observation ID, the exposure ID, the start of the observation, the exposure time (in seconds), taken from the ONTIME keyword, and the filter used.

Table A.2: (continued)

Obs ID	ExpID	Date start	Ontime	Mode
0412980501	PNS001	2008-04-19T09:27:21.525	29367	Thin1
	M1S002	2008-04-19T09:21:54.513	29565	Thin1
	M2S003	2008-04-19T09:21:54.513	29559	Thin1
0412980701	M1S002	2008-11-14T19:48:41.122	28569	Thin1
	M2S003	2008-11-14T19:48:41.122	28573	Thin1
0412980801	PNS001	2009-04-13T00:08:49.731	28398	Thin1
	M1S002	2009-04-13T00:03:23.718	28600	Thin1
	M2S003	2009-04-13T00:03:23.718	28600	Thin1
0412980901	M1S002	2009-10-21T09:04:02.437	28600	Thin1
	M2S003	2009-10-21T09:04:02.437	28600	Thin1
0412981001	PNS001	2010-04-21T01:41:11.495	30000	Thin1
	M1S002	2010-04-21T01:35:45.482	30200	Thin1
	M2S003	2010-04-21T01:35:45.482	30200	Thin1
0412981301	M1S002	2010-10-18T21:42:28.952	7048	Thin1
	M1U002	2010-10-19T00:22:52.640	21994	Thin1
	M2S003	2010-10-18T21:42:28.952	7079	Thin1
0412981401	M2U002	2010-10-19T00:22:59.640	21995	Thin1
	PNS001	2011-04-20T23:45:51.674	34600	Thin1
0412981501	M1S002	2011-04-20T23:40:25.660	34800	Thin1
	M2S003	2011-04-20T23:40:25.660	34800	Thin1
0412981601	M2U002	2011-11-04T18:40:40.206	28700	Medium
	PNS001	2012-12-06T16:27:27.059	14899	Thin1
0412981701	PNS012	2012-12-06T21:01:24.564	16685	Medium
	PNS013	2012-12-07T02:05:21.973	20883	Thick
0412982101	M1S002	2012-12-06T16:22:06.068	15200	Thin1
	M1S014	2012-12-06T20:47:06.591	16981	Medium
0412982201	M1S015	2012-12-07T01:42:05.019	24380	Thick
	M2S003	2012-12-06T16:22:06.068	15200	Thin1
0412982301	M2S016	2012-12-06T20:47:05.591	16983	Medium
	M2S017	2012-12-07T01:42:06.019	11500	Thick
0412982401	PNS001	2013-11-07T04:46:07.490	31694	Thin1
	M1S002	2013-11-07T04:40:18.504	31900	Thin1
0412982501	M2S003	2013-11-07T04:40:47.502	31888	Thin1
	PNS001	2014-10-20T08:12:59.834	33390	Medium
0412982601	M1S002	2014-10-20T08:07:09.848	33587	Thin1
	M2S003	2014-10-20T08:07:39.847	33589	Thin1
0412982701	M1S002	2014-10-20T18:10:28.279	43479	Thin1
	M2S003	2014-10-20T18:10:58.278	43477	Thin1
0412982801	PNS001	2015-10-30T17:01:28.666	37110	Medium
	M1S002	2015-10-30T16:55:38.682	37310	Thin1
0412982901	M2S003	2015-10-30T16:56:08.680	37282	Thin1
	M1S002	2015-10-28T18:08:45.639	33482	Thin1
0412983001	M2S003	2015-10-28T18:09:14.638	33483	Thin1
	PNS001	2016-10-26T23:24:23.019	35768	Medium
0412983101	M1S002	2016-10-26T23:18:53.031	35964	Thin1
	M2S003	2016-10-26T23:19:22.030	35962	Thin1
0412983201	M1S002	2016-12-03T18:37:33.517	33584	Thin1
	M2S003	2016-12-03T18:38:02.516	33588	Thin1
0791580701	PNS001	2016-04-26T04:41:47.236	30397	Thick
	PNS001	2016-04-26T13:35:09.695	12399	Medium
0791580801	PNS001	2016-04-26T17:28:31.303	12400	Thin1
	PNS001	2016-04-26T21:21:51.894	30400	Thick
0791581101	PNS001	2016-04-27T06:15:12.184	14088	Medium
	PNS001	2016-04-27T10:36:52.779	17400	Thin1

Table A.3: Summary of the Chandra observations used in this work (see text for more details).

Set	Obs ID	DetNam	Date start	Ontime	DataMode
1	138	ACIS-235678	1999-08-23T16:04:07	9757	FAINT
	1231	ACIS-235678	1999-08-23T19:18:41	9760	FAINT
2	134	ACIS-012367	1999-08-27T10:51:54	9754	FAINT
	1234	ACIS-012367	1999-08-27T13:59:32	9759	FAINT
3	120	ACIS-456789	1999-09-28T22:35:15	88208	FAINT
4	968	ACIS-456789	1999-10-08T20:58:01	49035	FAINT
5	1423	ACIS-56789	1999-11-01T16:09:36	19162	FAINT
6	48	ACIS-01236	2000-01-17T18:34:47	8678	FAINT
	49	ACIS-01236	2000-01-17T21:31:53	9270	FAINT
7	420	ACIS-012367	2000-03-14T02:32:29	10396	VFAINT
8	136	ACIS-012367	2000-03-16T04:17:31	10051	FAINT
9	140	ACIS-012367	2000-04-04T05:52:37	8345	FAINT
	439	ACIS-012367	2000-04-04T08:30:34	6954	FAINT
	440	ACIS-012367	2000-04-04T10:43:54	6955	FAINT
10	444	ACIS-012367	2000-04-30T08:20:31	8479	FAINT
	445	ACIS-012367	2000-04-30T11:01:42	8022	FAINT
11	141	ACIS-235678	2000-05-28T08:56:05	9833	FAINT
	1702	ACIS-235678	2000-05-28T12:07:21	9632	FAINT
12	1803	ACIS-235678	2000-07-03T00:59:24	8083	FAINT
	1789	ACIS-235678	2000-07-03T03:36:02	7674	FAINT
	1783	ACIS-012367	2000-07-03T05:56:32	7869	FAINT
	1784	ACIS-012367	2000-07-03T08:36:32	7674	FAINT
	1785	ACIS-012367	2000-07-03T10:57:02	7680	FAINT
	1786	ACIS-012367	2000-07-03T13:17:33	7680	FAINT
	1787	ACIS-012367	2000-07-03T15:38:02	7690	FAINT
13	1308	ACIS-235678	2000-12-10T06:17:32	7955	FAINT
	1311	ACIS-235678	2000-12-10T08:53:25	7754	FAINT
	1312	ACIS-235678	2000-12-10T11:15:14	7757	FAINT
	1478	ACIS-456789	2000-12-10T13:37:05	7948	FAINT
	1510	ACIS-456789	2000-12-10T16:18:25	7754	FAINT
	1525	ACIS-456789	2000-12-10T18:40:14	7757	FAINT
	1526	ACIS-456789	2000-12-10T21:02:04	7757	FAINT
14	1314	ACIS-012367	2000-12-15T13:57:20	6954	FAINT
	1315	ACIS-012367	2000-12-15T16:05:49	6957	FAINT
	1316	ACIS-012367	2000-12-15T18:14:19	6957	FAINT
	1317	ACIS-012367	2000-12-15T20:22:49	6957	FAINT
	1527	ACIS-012367	2000-12-15T22:31:18	6960	FAINT
	1528	ACIS-012367	2000-12-16T00:39:48	6960	FAINT
	1529	ACIS-012367	2000-12-16T02:48:18	6960	FAINT
15	1530	ACIS-235678	2001-06-06T01:12:14	7704	FAINT
	1531	ACIS-235678	2001-06-06T03:49:14	7507	FAINT
	1532	ACIS-235678	2001-06-06T06:07:00	7514	FAINT
	1533	ACIS-012367	2001-06-05T06:36:47	7510	FAINT
	1534	ACIS-012367	2001-06-05T09:01:21	7514	FAINT
	1535	ACIS-012367	2001-06-05T11:19:06	7504	FAINT
	1536	ACIS-012367	2001-06-05T13:36:52	7510	FAINT
	1537	ACIS-012367	2001-06-05T15:56:14	7513	FAINT
	1538	ACIS-456789	2001-06-06T08:24:45	7706	FAINT
	1539	ACIS-456789	2001-06-06T11:02:00	7510	FAINT
	1540	ACIS-456789	2001-06-06T13:19:45	7514	FAINT
	1541	ACIS-456789	2001-06-06T15:37:31	7514	FAINT
	1542	ACIS-012367	2001-06-05T18:17:10	7514	FAINT
	1543	ACIS-012367	2001-06-05T20:36:29	7514	FAINT
	1544	ACIS-012367	2001-06-05T22:54:13	7510	FAINT
16	2836	ACIS-012367	2001-12-05T14:37:53	7552	FAINT
	2837	ACIS-012367	2001-12-05T16:56:22	7558	FAINT
	2838	ACIS-012367	2001-12-05T19:14:52	7558	FAINT
	2839	ACIS-012367	2001-12-05T21:33:22	7558	FAINT
	2840	ACIS-012367	2001-12-05T23:51:51	7558	FAINT
	2841	ACIS-012367	2001-12-06T02:10:21	7558	FAINT
	2842	ACIS-012367	2001-12-06T04:28:51	7558	FAINT
	2843	ACIS-235678	2001-12-06T06:47:36	7760	FAINT
	2844	ACIS-235678	2001-12-06T09:25:20	7552	FAINT
	2845	ACIS-235678	2001-12-06T11:43:50	7558	FAINT
17	2846	ACIS-456789	2001-12-08T23:16:07	7949	FAINT
	2847	ACIS-456789	2001-12-09T01:46:57	7552	FAINT
	2848	ACIS-456789	2001-12-09T04:05:27	7558	FAINT
	2849	ACIS-456789	2001-12-09T06:23:56	7302	FAINT
18	2850	ACIS-235678	2002-06-19T16:25:39	7859	FAINT
	2851	ACIS-235678	2002-06-19T18:59:01	7654	FAINT
	2852	ACIS-235678	2002-06-19T21:20:25	7661	FAINT

**Notes.** Columns 3 to 5 list the time of the start of the observation, the exposure time (in seconds), taken from the ONTIME keyword, and the Observing Mode (Faint and Very Faint format, where pixel values are read out from a 3x3 or 5x5 region surrounding the event, respectively).

Table A.3: (continued)

Set	Obs ID	DetNam	Date start	Ontime	DataMode	Set	Obs ID	DetNam	Date start	Ontime	DataMode	
19	2857	ACIS-012367	2002-06-21T02:11:35	7651	FAINT	40	6057	ACIS-012367	2004-12-17T22:47:29	7955	VFAINT	
	2858	ACIS-012367	2002-06-21T04:39:09	7654	FAINT		6075	ACIS-456789	2004-12-18T01:21:24	7955	VFAINT	
	2859	ACIS-012367	2002-06-21T06:59:19	7658	FAINT	41	6076	ACIS-456789	2004-12-19T10:52:37	7952	VFAINT	
	2860	ACIS-012367	2002-06-21T09:19:30	7654	FAINT		6077	ACIS-456789	2004-12-19T13:26:12	7754	VFAINT	
	2862	ACIS-012367	2002-06-21T13:59:50	7658	FAINT		6078	ACIS-456789	2004-12-19T15:48:02	7757	VFAINT	
	2863	ACIS-012367	2002-06-21T16:20:00	7658	FAINT	42	6079	ACIS-456789	2004-12-20T08:06:36	7955	VFAINT	
	2864	ACIS-012367	2002-06-21T18:40:10	7658	FAINT		6080	ACIS-456789	2004-12-20T10:38:29	7753	VFAINT	
20	2853	ACIS-456789	2002-06-22T06:20:31	7856	FAINT	43	6051	ACIS-012367	2005-01-12T04:25:55	18150	VFAINT	
	2854	ACIS-456789	2002-06-22T08:52:42	7654	FAINT		6053	ACIS-012367	2005-01-12T09:49:06	7254	VFAINT	
	2855	ACIS-456789	2002-06-22T11:12:52	7658	FAINT		6054	ACIS-012367	2005-01-12T12:02:36	7258	VFAINT	
	2856	ACIS-456789	2002-06-22T13:34:30	7660	FAINT	44	6042	ACIS-456789	2005-04-12T01:40:22	19146	VFAINT	
21	3828	ACIS-456789	2002-12-20T14:48:39	137658	FAINT		6043	ACIS-456789	2005-04-18T08:43:21	7952	VFAINT	
22	3519	ACIS-235678	2003-02-01T04:33:34	8112	VFAINT		6060	ACIS-012367	2005-06-13T13:12:55	20058	VFAINT	
	3520	ACIS-235678	2003-02-01T07:06:41	7728	VFAINT	47	6750	ACIS-012367	2006-03-14T08:41:34	7603	VFAINT	
	3521	ACIS-235678	2003-02-01T09:28:04	7731	VFAINT		6751	ACIS-012367	2006-03-14T11:13:46	7254	VFAINT	
	3523	ACIS-235678	2003-02-01T11:49:27	7731	VFAINT		6752	ACIS-012367	2006-03-14T13:27:16	7254	VFAINT	
	3524	ACIS-235678	2003-02-01T14:10:50	7728	VFAINT		6753	ACIS-012367	2006-03-14T15:40:47	7258	VFAINT	
	3522	ACIS-456789	2003-02-01T16:32:13	7933	VFAINT		6754	ACIS-012367	2006-03-14T17:54:17	7254	VFAINT	
	3525	ACIS-456789	2003-02-01T19:13:06	7728	VFAINT		6755	ACIS-012367	2006-03-14T20:07:47	7254	VFAINT	
	3535	ACIS-012367	2003-02-02T12:34:29	7935	VFAINT	48	6758	ACIS-456789	2006-03-19T04:28:05	8163	VFAINT	
	3536	ACIS-012367	2003-02-02T00:15:22	7725	VFAINT		6760	ACIS-456789	2006-03-19T07:01:31	7753	VFAINT	
	3537	ACIS-012367	2003-02-02T02:36:45	7731	VFAINT		6761	ACIS-456789	2006-03-19T09:23:21	7757	VFAINT	
	3538	ACIS-012367	2003-02-02T04:58:08	7731	VFAINT		6762	ACIS-456789	2006-03-19T11:45:11	7757	VFAINT	
	3539	ACIS-012367	2003-02-02T07:19:31	7731	VFAINT		6763	ACIS-456789	2006-03-19T14:07:01	7754	VFAINT	
	3540	ACIS-012367	2003-02-02T09:40:54	7731	VFAINT		6764	ACIS-456789	2006-03-19T16:28:52	7757	VFAINT	
	3541	ACIS-012367	2003-02-02T12:02:17	7731	VFAINT	49	6759	ACIS-456789	2006-03-21T23:28:29	18141	VFAINT	
	3542	ACIS-012367	2003-02-02T14:23:40	7731	VFAINT		6748	ACIS-012367	2006-03-22T11:47:51	7951	VFAINT	
	3543	ACIS-012367	2003-02-02T16:45:03	7738	VFAINT	51	6747	ACIS-012367	2006-04-03T05:23:29	7376	VFAINT	
23	3526	ACIS-012367	2003-08-05T22:31:32	8181	VFAINT		6757	ACIS-012367	2006-05-06T13:19:43	20058	VFAINT	
	3527	ACIS-012367	2003-08-06T01:03:11	7965	VFAINT		6766	ACIS-456789	2006-06-06T13:28:51	19949	VFAINT	
24	3546	ACIS-235678	2003-08-08T17:58:11	7962	VFAINT		8361	ACIS-012367	2007-02-05T02:20:53	20045	VFAINT	
	3547	ACIS-235678	2003-08-08T20:39:32	7754	VFAINT		8366	ACIS-235678	2007-02-08T13:43:28	8342	VFAINT	
	3548	ACIS-235678	2003-08-08T23:01:21	7754	VFAINT		8367	ACIS-235678	2007-02-08T16:22:01	7955	VFAINT	
	3528	ACIS-012367	2003-08-09T01:23:12	7962	VFAINT	56	8362	ACIS-012367	2007-02-11T08:13:03	8957	VFAINT	
	3529	ACIS-012367	2003-08-09T04:04:31	7750	VFAINT		8363	ACIS-012367	2007-02-11T11:00:38	8553	VFAINT	
	3530	ACIS-012367	2003-08-09T06:26:21	7750	VFAINT		8364	ACIS-012367	2007-02-11T13:35:48	8557	VFAINT	
25	3532	ACIS-012367	2003-08-10T09:07:04	7750	VFAINT	57	9691	ACIS-01236	2008-02-04T23:02:12	8045	VFAINT	
	3533	ACIS-012367	2003-08-10T11:28:53	7757	VFAINT		9692	ACIS-01236	2008-02-05T01:42:29	7774	VFAINT	
	3534	ACIS-012367	2003-08-10T13:50:44	7757	VFAINT		9693	ACIS-01236	2008-02-05T04:04:18	7777	VFAINT	
	3544	ACIS-235678	2003-08-10T16:12:49	7962	VFAINT	58	9695	ACIS-35678	2008-02-07T13:58:22	8032	VFAINT	
26	5123	ACIS-456789	2003-12-15T04:24:59	20582	VFAINT		9696	ACIS-35678	2008-02-07T16:38:39	7774	VFAINT	
	5124	ACIS-456789	2003-12-15T10:30:54	8003	VFAINT	59	10652	ACIS-01236	2009-01-17T20:41:03	8175	VFAINT	
	5125	ACIS-456789	2003-12-15T12:56:53	8010	VFAINT		60	10650	ACIS-01236	2009-02-16T18:17:32	8038	VFAINT
	5126	ACIS-456789	2003-12-15T15:22:54	8010	VFAINT		61	10651	ACIS-01236	2009-02-17T07:38:59	8043	VFAINT
	5127	ACIS-456789	2003-12-15T17:48:53	8010	VFAINT		62	12147	ACIS-456789	2011-02-11T17:01:11	150794	FAINT
	5128	ACIS-456789	2003-12-15T20:14:53	8006	VFAINT		63	13411	ACIS-5	2011-05-23T02:29:16	10028	VFAINT
	5129	ACIS-456789	2003-12-15T22:40:53	8010	VFAINT	64	13409	ACIS-5	2011-05-28T01:40:18	10028	VFAINT	
27	5153	ACIS-012367	2003-12-16T22:24:48	7491	VFAINT		13410	ACIS-5	2011-05-28T04:45:17	10028	VFAINT	
	5154	ACIS-012367	2003-12-17T00:53:15	7546	VFAINT	65	17687	ACIS-3	2015-07-18T02:35:28	13966	VFAINT	
28	5147	ACIS-012367	2003-12-19T01:55:58	8032	VFAINT		66	18419	ACIS-7	2016-03-22T05:39:25	20063	VFAINT
	5148	ACIS-012367	2003-12-19T04:39:08	19529	VFAINT							
	5149	ACIS-012367	2003-12-19T10:17:19	7667	VFAINT							
	5150	ACIS-012367	2003-12-19T12:37:42	7670	VFAINT							
	5151	ACIS-012367	2003-12-19T14:58:05	7670	VFAINT							
29	5152	ACIS-012367	2003-12-22T07:45:55	8080	VFAINT							
30	5251	ACIS-456789	2003-12-24T20:43:02	7708	VFAINT							
	5252	ACIS-456789	2003-12-24T23:15:05	7549	VFAINT							
31	5131	ACIS-456789	2004-04-05T04:47:50	8115	VFAINT							
32	5130	ACIS-456789	2004-04-09T13:07:30	19661	VFAINT							
	5132	ACIS-456789	2004-04-09T18:55:24	7596	VFAINT							
	5133	ACIS-456789	2004-04-09T21:14:35	7597	VFAINT							
	5134	ACIS-456789	2004-04-09T23:33:45	7597	VFAINT							
33	5135	ACIS-456789	2004-04-10T12:34:32	8246	VFAINT							
	5136	ACIS-456789	2004-04-10T15:35:17	8041	VFAINT							
	5139	ACIS-012367	2004-04-10T18:01:57	20682	VFAINT							
34	5143	ACIS-012367	2004-04-26T10:49:08	7443	VFAINT							
	5144	ACIS-012367	2004-04-26T13:14:00	7235	VFAINT							
	5145	ACIS-012367	2004-04-26T15:27:11	7238	VFAINT							
35	5137	ACIS-012367	2004-04-28T00:27:20	8141	VFAINT							
	5138	ACIS-012367	2004-04-28T03:02:20	7754	VFAINT							
36	5140	ACIS-012367	2004-04-30T16:57:40	8144	VFAINT							
	5141	ACIS-012367	2004-04-30T19:32:39	7754	VFAINT							
	5142	ACIS-012367	2004-04-30T21:54:29	7757	VFAINT							
37	6050	ACIS-012367	2004-12-13T03:35:35	7254	VFAINT							
38	6052	ACIS-012367	2004-12-14T08:58:26	7642	VFAINT							
39	6074	ACIS-456789	2004-12-16T18:02:39	20099	VFAINT							
	6055	ACIS-012367	2004-12-16T23:56:21	7955	VFAINT							